Systematics of shape resonances in reactive collisions

Kazuhiro Sakimoto

Institute of Space and Astronautical Science, Japan Aerospace Exploration Agency, Yoshinodai 3-1-1, Chuo-ku, Sagamihara 252-5210, Japan

(Received 5 April 2016; revised manuscript received 18 August 2016; published 3 October 2016)

Wentzel-Kramers-Brillouin (WKB) methodology is used to undertake a systematic analysis of shape resonances in exoergic reactive collisions at low energies E, and examples investigated are $Li + H^+$, $He(2\,^3S) + H$, and $He(2\,^3S) + Mu$ (muonium). In so doing, the resonance positions should be measured by the tunneling parameter α and not by E. The resonance peak height P_{res} of the reaction probability and the resonance width times the vibrational period of the quasibound resonance state can be given by simple closed-form expressions with two variables, α and P_0, the latter of which is a reaction probability given at collision energies much above a centrifugal barrier top and is determined by only short-range interactions. The resonance promotes the reaction maximally (i.e., $P_{res} = 1$) when the resonance satisfies $\alpha = \alpha_0 = (2\pi)^{-1} \ln[(1 - P_0)/P_0]$, in other words, when the transmission coefficient of tunneling through the centrifugal barrier happens to be equal to P_0 at the resonance energy. If $\alpha_0 \gtrsim 1$, the reaction system is rich in tunneling resonances. If $\alpha_0 \lesssim 0$, the prominent resonances are mostly an over-barrier type. The resonances occurring at $\alpha \gg \alpha_0$ are of no significance in the reaction.

DOI: 10.1103/PhysRevA.94.042701

I. INTRODUCTION

A centrifugal barrier plays a key role in low-energy atomic collisions. Shape resonances in collisions are associated with quasibound motion trapped behind the centrifugal barrier and are characterized as a quantum-mechanical (QM) phenomenon. The shape resonance can make a dramatic change in the feature of reactive collisions as well as elastic and inelastic collisions. Such effects have indeed been confirmed in detailed experimental studies for various types of collision processes [1–12]. In classical mechanics, only when the collision energy E is higher than the centrifugal barrier can the two colliding particles come sufficiently close to each other. The frequency of such close encounters in collisions is proportional to the cross section $\sigma_0 = \pi b_0^2$, with b_0 being the impact parameter at which the collision energy is equal to the barrier height [13]. In the ion-molecule system, this cross section is often replaced with the Langevin cross section σ_L, obtained by assuming only the asymptotic polarization interaction. If, further, the reaction is exoergic and occurs only through short-range interactions inside the centrifugal barrier, the classical cross section for reaction may be given by $\sigma = \kappa\sigma_0$, where the reaction efficiency κ should be $0 \leqslant \kappa \leqslant 1$. Accordingly, if the collision system has very low reaction efficiency ($\kappa \ll 1$), the reaction cross section remains always much smaller than σ_0 in the classical picture. However, the QM phenomenon of the shape resonance especially due to tunneling through the centrifugal barrier is able to bring about a drastic increase in the reaction cross section from the classical value.

An example of revealing very low reaction efficiency and demonstrating the significance of shape resonances is found in the radiative reaction (radiative charge transfer plus radiative association) in $Li + H^+$ collisions. Figure 1 shows the reaction cross sections σ and the reaction probabilities P ($0 \leqslant P \leqslant 1$) for each partial wave in $Li + H^+$ at collision energies $E =$ 0.001–0.1 eV. These results were obtained by carrying out QM collision calculations in the present study (see later). The cross section σ and the probability P are related by

$$\sigma(E) = \frac{\pi\hbar^2}{2mE} \sum_L (2L + 1)P(E,L), \tag{1}$$

where m is the reduced mass of the collision system and L is the total angular momentum quantum number of the collision system. One can see plenty of shape resonances, which vary widely in a profile. In the energy range shown in Fig. 1, the resonances are observed for the partial waves $L =$ 21–62. It is found that the nonresonance part of the reaction cross section is nicely estimated by $\kappa\sigma_L$, with $\kappa = 10^{-5}$, and that the nonresonance reaction probabilities are $P \lesssim 10^{-5}$. Although this system reveals very low reaction efficiency, interestingly, the reaction probabilities for several resonances become considerably large (namely, very close to the upper limit $P = 1$).

In view of these facts, the following issues may be raised for exoergic reactive collisions. What conditions does the shape resonance satisfy when the reaction probability can reach ~1? Is there any means or regularity for arranging a systematical understanding of a vast variety of shape resonances? Usually, the profile of the shape resonance in the reaction remains unknown until a detailed QM calculation is carried out for the collisions. Is it possible to measure the importance of each resonance without such a collision calculation? For elastic collisions, by introducing Wentzel-Kramers-Brillouin (WKB) approximation and connection formulas, shape resonances have been investigated [14–16], and an analytical formula for the S matrix has been derived [17]. An elegant approach has been developed for reactive collisions by using the idea of quantum defect theory (QDT), and it has been applied to ultracold collisions [18–20]. Systematic studies of shape resonances with respect to molecular parameters have been made [21,22]. As far as the present author knows, however, the above issues concerning reactive collisions have not yet been resolved satisfactorily. Very recently, on the basis of the WKB approximation, the present author [23] obtained a versatile

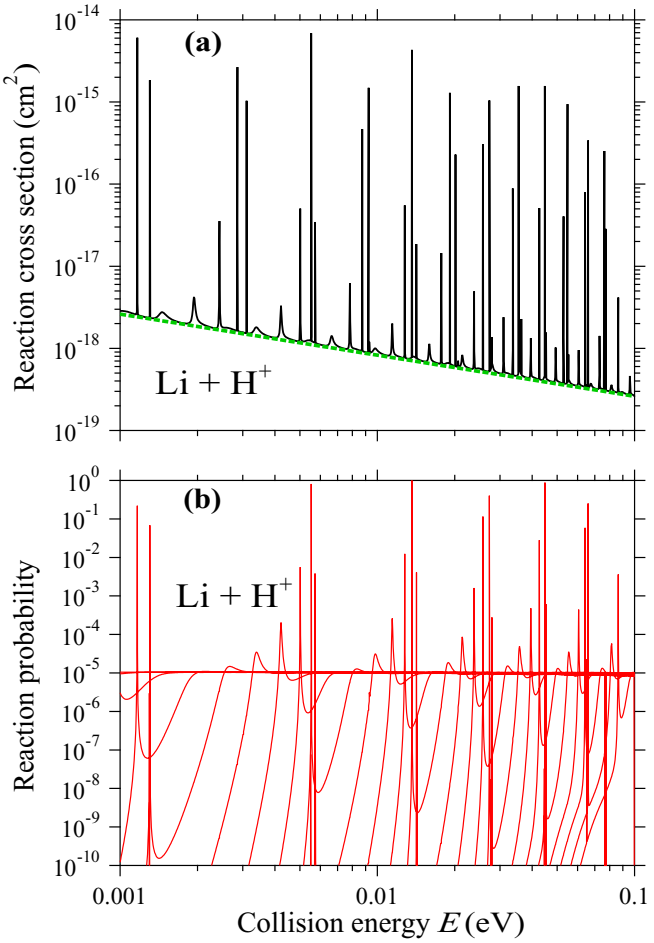

FIG. 1. (a) Reaction cross sections $\sigma(E)$ and (b) reaction probabilities $P(E,L)$ in $Li + H^+$ collisions, obtained with the present QM calculation, are shown at collision energies $E = 0.001$–0.1 eV. In (a), the solid line is the QM result, and the dashed line indicates $\kappa\sigma_L$, where σ_L is the Langevin cross section and $\kappa = 10^{-5}$ is the reaction efficiency. In (b), the QM results are shown only for odd L between 15 and 61 for brevity.

formula for the reaction probability including a complete expression of a resonance profile (this study is referred to as paper I herein). This formula is expected to be useful for examining the above issues.

The present paper proposes a way of systematically looking at the shape resonances in exoergic reactive collisions with the help of the WKB methodology developed in paper I. As examples, the shape resonances in two types of reaction processes are comprehensively investigated. One is the already-mentioned radiative reaction in the ion-molecule system $Li + H^+$, which has very low reaction efficiency ($\kappa = 10^{-5}$). The other is the autoionization reaction (leading to Penning ionization and associative ionization) in the neutral system $He(2\,^3S) + H$, which has high reaction efficiency ($\kappa \sim 0.8$), and in its isotope system $He(2\,^3S) + Mu$ ($\kappa \sim 0.4$), with Mu being a muonium atom. The hypothetical system of $He(2\,^3S) + H$, in which the reaction efficiency is adjusted to be low ($\kappa \sim 0.01$), is also considered. Of particular note is that it has become possible to investigate the shape resonances in experimental measurements for both radiative reaction

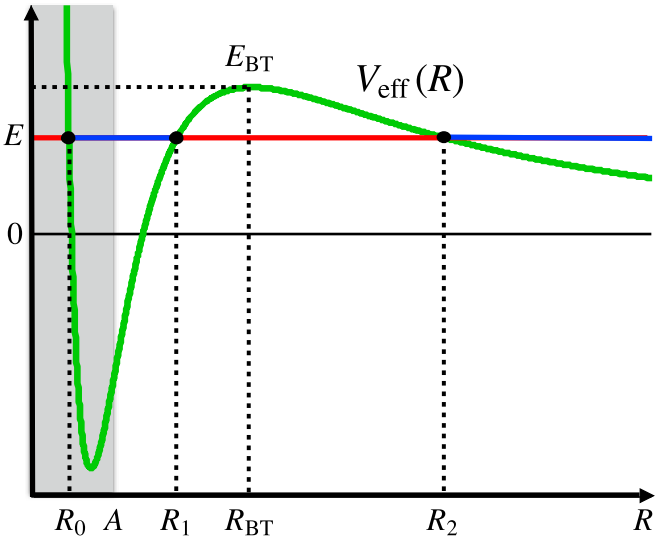

FIG. 2. A typical example of the interactions in atomic collisions. The effective potential $V_{\rm eff}(R)$ of the elastic channel, i.e., Eq. (4), is shown. The reactive interaction U zone localized at distances $R < A$ is distinguished by gray shading. The barrier top located at $R = R_{\rm BT}$ is indicated by $E_{\rm BT}$. For the collision energy $E < E_{\rm BT}$, there can be two classical turning points, R_1 and R_2. If $|U| \ll |V|$, the innermost turning point R_0 can be evaluated directly from $V_{\rm eff}(R)$.

and Penning ionization [3–5,8,11]. These reaction processes can be theoretically described by a local-complex-potential model [24,25]. In the present study, a search for resonances was made by carrying out the QM calculation of collisions governed by the local complex potential, and an R-matrix propagation method [26] was employed as a numerical solution technique.

The present paper is organized as follows: Sec. II gives the outline of the WKB method developed in paper I and reports some additional developments which are necessary for the present purpose. In Sec. III, the results of the QM collision calculations are presented, and a systematic analysis of the shape resonances found in the QM calculations is performed. Finally, Sec. IV gives the summary of the present study.

II. WKB APPROACH

The interactions in the collision systems considered in this study are schematically illustrated in Fig. 2. Let R be the radial distance between the collision pair. The reactive interaction U in the collision system is assumed to have a short range A. Beyond this range ($R > A$), the relative motion of the collision is assumed to be governed by only a spherically symmetric local potential $V(R)$, and hence, the radial wave function $G(R)$ for each partial wave L satisfies the following Schrödinger equation:

$$\left[\frac{d^2}{dR^2} + k^2(R)\right] G(R) = 0, \tag{2}$$

where

$$k^2(R) = \frac{2m}{\hbar^2}[E - V_{\rm eff}(R)], \tag{3}$$

with

$$V_{\rm eff}(R) = \frac{L(L+1)\hbar^2}{2mR^2} + V(R). \tag{4}$$

Unless L is too high, the effective potential $V_{\rm eff}(R)$ has a barrier top $E_{\rm BT}$ at $R = R_{\rm BT}$. When the collision energy E is below this barrier top, two classical turning points, R_1 and R_2, i.e., $k(R_1) = k(R_2) = 0$, can exist. In this study, it is reasonably assumed that $A < R_1 < R_2$. Even if the energy is $E > E_{\rm BT}$, one can introduce two complex-valued turning points $R_1 = (R_2)^*$, which are the roots of $k(R) = 0$.

To take into account the centrifugal-barrier effects in a manageable manner, the WKB approximation is employed for the solution of Eq. (2). On the inside of the centrifugal barrier ($A < R \ll R_{\rm BT}$), the wave function $G(R)$ can be expressed in terms of the WKB solutions [23]:

$$G(R) = \frac{C}{\sqrt{k(R)}} \exp\left\{+i\left[\int_R^{R_1} k(R')dR' + \frac{\pi}{4}\right]\right\} - \chi \frac{C}{\sqrt{k(R)}} \exp\left\{-i\left[\int_R^{R_1} k(R')dR' + \frac{\pi}{4}\right]\right\}, \tag{5}$$

where C is a constant. The complex-valued coefficient χ represents the collision information concerning the reactive interaction zone ($R < A$). Since the reaction leads to the loss of flux in the elastic channel, χ is not necessarily unitary (i.e., $|\chi|^2 \leqslant 1$) and can be generally written as

$$\chi = e^{-\eta + i\delta}, \tag{6}$$

where $\eta \geqslant 0$ and δ are real valued. As in paper I, it is useful to define the reactivity P_0 of the system for each partial wave L:

$$P_0 = 1 - |\chi|^2 = 1 - e^{-2\eta}, \tag{7}$$

which has the range of $0 \leqslant P_0 \leqslant 1$. The reactivity is not the reaction probability in the collision process but can be considered the inherent reactive ability of the system, which is determined by only the short-range interactions at $R < A$, without including the centrifugal-barrier effect. (The relation to the reaction efficiency κ will be discussed later.) Also, in the QDT treatment, the reactivity is introduced as a short-range parameter [18–20]. Especially if one can assume $|U| \ll |V|$ (or, equivalently, $P_0 \ll 1$), the relative motion is practically governed by $V(R)$ at all distances R (even at $R < A$), and the phase δ can be calculated by

$$\delta = 2\int_{R_0}^{R_1} k(R)dR + \pi, \tag{8}$$

where R_0 is the innermost turning point other than R_1 and R_2, i.e., $k(R_0) = 0$ [23].

On the outside of the centrifugal barrier (i.e., $R \gg R_{\rm BT}$), the wave function $G(R)$ can be written as

$$G(R) = \frac{C'}{\sqrt{k(R)}} \exp\left\{-i\left[\int_{R_2}^{R} k(R')dR' + \frac{\pi}{4}\right]\right\} - S \frac{C'}{\sqrt{k(R)}} \exp\left\{+i\left[\int_{R_2}^{R} k(R')dR' + \frac{\pi}{4}\right]\right\}, \tag{9}$$

where C' is a constant. Since Eq. (9) is valid also in the limit $R \to \infty$, the coefficient S (without an unimportant phase factor) can be regarded as the elastic part of the S matrix in the collision process. Applying the connection formula based on parabolic cylinder functions [16,27] to Eq. (5) and then comparing the result with Eq. (9), paper I shows

$$S = \frac{e^{\pi\alpha - i\phi} - \chi\sqrt{1+e^{2\pi\alpha}}}{\chi e^{\pi\alpha + i\phi} - \sqrt{1+e^{2\pi\alpha}}}, \tag{10}$$

where

$$\alpha = -\frac{i}{\pi}\int_{R_1}^{R_2} k(R)dR \tag{11}$$

is the tunneling parameter [16,27], and

$$\phi = \arg\Gamma\left(\frac{1}{2} + i\alpha\right) + \alpha(1 - \ln|\alpha|) \tag{12}$$

represents the phase correction due to the centrifugal-barrier effect. The parameters α, ϕ, and χ in Eq. (10) depend on the collision energy E and also on L. The tunneling parameter becomes $\alpha > 0$ at $E < E_{\rm BT}$, $\alpha = 0$ at $E = E_{\rm BT}$, and $\alpha < 0$ at $E > E_{\rm BT}$. The correction ϕ is not large and is always $|\phi| < 0.024$.

A. Reaction probability

When χ is not unitary ($\eta > 0$), Eq. (10) is not unitary either, i.e., $|S|^2 < 1$. One can regard $P = 1 - |S|^2$ precisely as the reaction probability in the collision process. From Eqs. (6), (7), and (10), the reaction probability for given E and L can be expressed as

$$P(E,L) = F[\alpha(E,L), \theta(E,L), P_0(E,L)], \tag{13}$$

where

$$F(\alpha,\theta,P_0) = \frac{e^{-2\pi\alpha}P_0}{2 + e^{-2\pi\alpha} - P_0 - 2\cos\theta\sqrt{(1+e^{-2\pi\alpha})(1-P_0)}} \tag{14}$$

and a new parameter θ is defined by $\theta = \delta + \phi$. A similar WKB treatment was employed for reactive collisions by Jachymski *et al.* [19]. However, the expressions for Eqs. (10) and (14) were not derived there. The probability function $F(\alpha,\theta,P_0)$ has explicit dependence neither on the other system parameters (m, L, and E) nor on the details of the interaction. Thus, all the possible profiles of the resonance and nonresonance reaction probabilities are expressible for an arbitrary reaction system by this simple universal formula which has only three real-valued parameters (α,θ,P_0). In the limit $\alpha \to -\infty$,

$$F(\alpha,\theta,P_0) \to P_0. \tag{15}$$

Namely, one can have $P_0(E,L) = P(E,L)$ at $E \gg E_{\rm BT}$. In many cases, the reactivity $P_0(E,L)$ can be considered to be actually independent of E and has a slight dependence on L [18–20,23]. Figure 3 shows the L dependence of the reactivity P_0, which is calculated by assuming $P_0 = P(E,L)$ at $E = 0.1$ eV in the present QM calculations of the $Li + H^+$ and $He(2\,^3S) + H$ systems (see below). Since the variation with L is not so large in the related range of L, the reactivity may be reasonably considered to be an L-independent parameter. Then, one can postulate $P_0 \simeq \kappa$ [19,23], and the reactivity P_0 can be estimated experimentally because the nonresonance

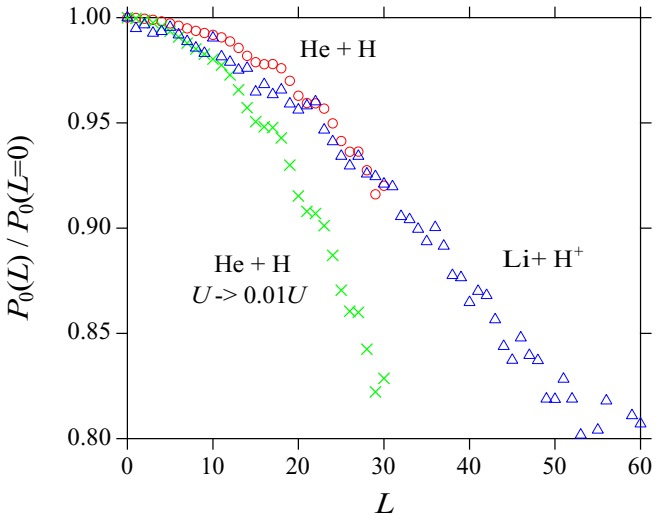

FIG. 3. L dependence of $P_0(L)/P_0(L=0)$ for the reactions in $Li + H^+$ (triangles) and $He(2\,^3S) + H$ (circles), obtained with the present QM calculation. Also shown is the result for the hypothetical $He(2\,^3S) + H$ system (crosses), in which the reactive interaction U is replaced with $0.01U$.

part of the reaction cross section is given by the classical cross section $\kappa\sigma_0 \simeq P_0\sigma_0$. Hereafter, the probability function F is defined as a two-independent-variable function, i.e., $F(\alpha,\theta)$, with a constant parameter P_0.

In paper I, the mathematical property of $F(\alpha,\theta)$ was investigated by assuming that α and θ are independent variables. This is very useful for understanding general characteristics and any conceivable profiles of shape resonances. The probability function $F(\alpha,\theta)$ forms a topographical map on the α-θ plane. Figure 4(a) illustrates the contour plot of $F(\alpha,\theta)$ for $P_0 = 10^{-5}$, which corresponds to the case of the $Li + H^+$ system. (It should be noted that α is arranged in descending order if it is chosen as the horizontal axis.) In this map, only the specific values of $F(\alpha,\theta)$ for the variables satisfying $(\alpha,\theta) = [\alpha(E,L),\theta(E,L)]$, which form a route on the topographical map in response to the energy variation for each fixed L [23], are recognized as the actual reaction probabilities $P(E,L)$. For the $Li + H^+$ collisions with $L = 39$, the energy dependences $\alpha(E)$ and $\theta(E)$ are shown in Figs. 4(b) and 4(c). (Hereafter, the L dependence is not specified explicitly.) The corresponding route is drawn in Fig. 4(a). The topographical map always shows a ridge along the line given by $\cos\theta = 1$ irrespective of the value of $0 < P_0 < 1$. When the energy-variation route $[\alpha(E),\theta(E)]$ crosses over this ridge line, the reaction probability exhibits a peak (or shoulder) structure, which is due to a resonance. It should be noted that the shape resonance always has an additive (not destructive) profile. Figure 4(d) shows the reaction probability $P(E)$ obtained with the present QM calculation for the $Li + H^+$ collisions with $L = 39$. The positions of the resonance peaks almost coincide with the energy corresponding to $\cos\theta = 1$ on the route. Thus, the resonance peak position E_{res} can be set approximately equal to the ridge position satisfying

$$\theta(E) = 2n\pi, \tag{16}$$

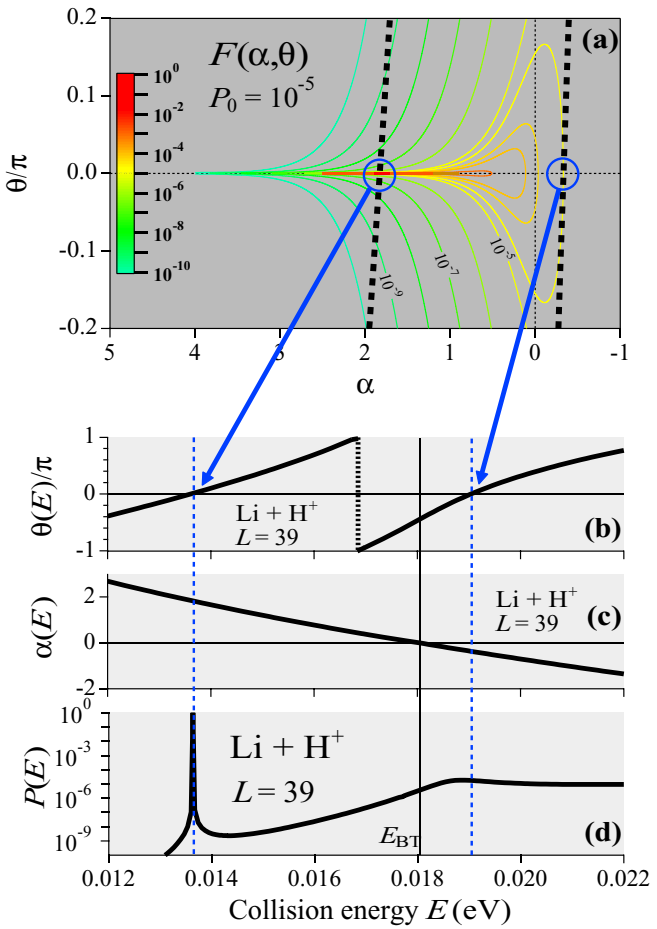

FIG. 4. (a) A contour plot of the probability function $F(\alpha,\theta)$ for the reactivity $P_0 = 10^{-5}$. The variable θ is expressed by mod 2π. Only the range $-0.2 \leqslant \theta/\pi \leqslant 0.2$ is drawn because the ridge ($\theta = 0$) is very narrow along θ. Dashed lines are the energy-variation route $[\alpha(E),\theta(E)/\pi]$ for the $Li + H^+$ collisions with $L = 39$. Circles indicate the $\theta = 0$ point on this route. (b) A plot of $\theta(E)/\pi$ (mod 2) against E for $Li + H^+$ with $L = 39$. (c) A plot of $\alpha(E)$ against E for $Li + H^+$ with $L = 39$. (d) Reaction probabilities $P(E)$, obtained with the present QM calculation, plotted against E for $Li + H^+$ with $L = 39$.

with n being an integer. In the special case of $|U| \ll |V|$, one can use Eq. (8) and then obtain

$$\int_{R_0}^{R_1} k(R)dR + \frac{\phi}{2} = \left(n + \frac{1}{2}\right)\pi, \tag{17}$$

which is the famous Bohr-Sommerfeld quantization rule (including the centrifugal-barrier effect).

B. Resonance peak

Paper I took into account the height of the ridge, which is given by

$$f(\alpha) = F(\alpha,\theta = 2n\pi) = \frac{e^{-2\pi\alpha}P_0}{(\sqrt{1 + e^{-2\pi\alpha}} - \sqrt{1 - P_0})^2}. \tag{18}$$

The probability peak height P_{res} of the resonance may be set equal to the value of this height function

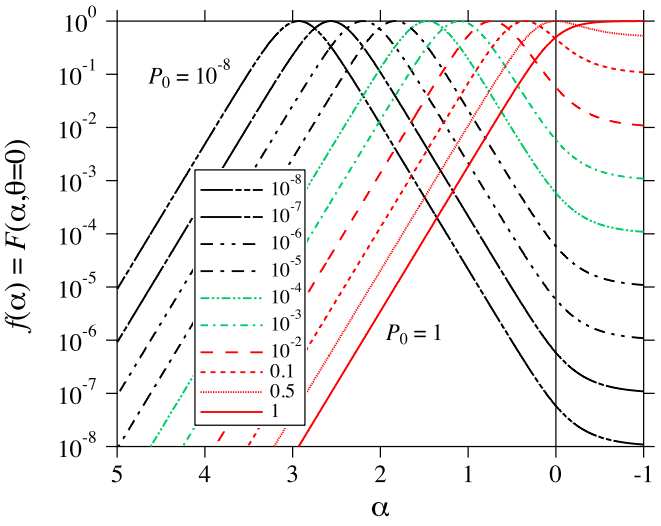

FIG. 5. Height functions $f(\alpha) = F(\alpha,\theta=0)$, i.e., Eq. (18), in the range of $5 \geqslant \alpha \geqslant -1$ for the reactivities $P_0 = 10^{-8}$–10^{0}. The function $f(\alpha)$ takes the maximum value (=1) at $\alpha = (2\pi)^{-1} \ln[(1 - P_0)/P_0]$.

$f(\alpha)$ at $\alpha = \alpha_{\rm res} = \alpha(E_{\rm res})$. Figure 5 shows $f(\alpha)$ for various reactivities P_0. As long as $P_0 \neq 0$ (even for extremely low $P_0 \ll 1$), the height function always has the maximum value of the upper limit (=1) when α becomes

$$\alpha_0 = \frac{1}{2\pi} \ln \frac{1 - P_0}{P_0}, \tag{19}$$

which is $\gtrless 0$ corresponding to $P_0 \lessgtr 0.5$. Equation (19) can be rewritten as

$$P_0 = \frac{1}{1 + e^{2\pi\alpha_0}}. \tag{20}$$

The right-hand side of Eq. (20) has the same form as the transmission coefficient obtained by applying the connection formula in the WKB method [27]. Therefore, it turns out that the resonance promotes the reaction to the uppermost limit if the transmission coefficient is accidentally equal to the reactivity at the resonance energy. For the $Li + H^+$ system ($P_0 = 10^{-5}$), one has $\alpha_0 = 1.832$, and the QM calculation [Fig. 4(d)] shows that the peak position of the tunneling resonance is $E_{\rm res} = 0.01364$ eV, which corresponds to $\alpha_{\rm res} = 1.831$. Accordingly, it is understandable that $P_{\rm res} \simeq 1$ for this resonance. The height function $f(\alpha)$ is monotonically decreasing as α increases from α_0, and the peak height becomes $P_{\rm res} < P_0$ for α larger than

$$\alpha_1 = \alpha_0 + \frac{1}{2\pi} \ln \frac{4}{P_0}. \tag{21}$$

In Fig. 5, the shape of $f(\alpha)$ around the maximum center $\alpha = \alpha_0$ seems to be exactly the same, especially for small P_0. In the case of $P_0 \ll 1$ and $e^{-2\pi\alpha} \ll 1$, the height function indeed becomes

$$f(\alpha) = \frac{1}{\cosh^2[\pi(\alpha - \alpha_0)]}, \tag{22}$$

which satisfies $f(\alpha_0 \pm \Delta\alpha_N) = f(\alpha_0)/N$, with $\Delta\alpha_N = \pi^{-1} \ln(\sqrt{N} + \sqrt{N-1})$.

The degree of ridge-peak prominence (how high the peak towers up along the θ direction) may be measured by

$$D(\alpha) = \frac{F(\alpha,\theta=0)}{F(\alpha,\theta=\pi)} = \left(\frac{\sqrt{1 + e^{-2\pi\alpha}} + \sqrt{1 - P_0}}{\sqrt{1 + e^{-2\pi\alpha}} - \sqrt{1 - P_0}} \right)^2, \tag{23}$$

which is $\geqslant 1$. A larger value of $D(\alpha)$ means that the ridge peak is more prominent. In the limit $\alpha \to \infty$, one has $D(\alpha) \sim 1$ for $P_0 \sim 1$ and $D(\alpha) = 16(P_0)^{-2} \gg 1$ for $P_0 \ll 1$. For the tunneling resonances occurring at $E_{\rm res} \ll E_{\rm BT}$, one can thus expect that the resonance profile becomes relatively much more prominent as P_0 decreases. It should be mentioned, however, that $D(\alpha)$ is not the degree of *resonance-peak prominence* because the resonance profile must actually be defined along the energy-variation route $[\alpha(E),\theta(E)]$. In the opposite limit $\alpha \to -\infty$, one has $F(\alpha,\theta) \to P_0$ irrespective of θ, and naturally, $D(\alpha) \to 1$. It is fairly obvious that no peak structure is observed at $E \gg E_{\rm BT}$. Figure 5 shows $f(\alpha) \sim P_0$ even at $\alpha \sim -1$, and hence, one can expect that the over-barrier resonances are prominent only for $\alpha \gtrsim -1$. If $\alpha_1 < 0$ [see Eq. (21)], then the peak height always becomes $P_{\rm res} < P_0$ for all the tunneling resonances, which means that the tunneling resonances are insignificant in the first place. The condition $\alpha_1 < 0$ gives $P_0 > 2(\sqrt{2} - 1) = 0.8284$ (or $\alpha_0 < -0.2506$), which was adopted in paper I as a criterion for judging that no clear tunneling resonance can be observed in the reaction.

C. Resonance width

The resonance energy $E_{\rm res}$ and the resonance energy width Γ are evaluated using the pole of the S matrix, i.e., $S(E_{\rm pol}) = \infty$, with $E_{\rm pol} = E_{\rm res} - i\Gamma/2$. From Eq. (10), the pole satisfies

$$\theta = 2n\pi - i\left[\eta + \tfrac{1}{2} \ln(1 + e^{-2\pi\alpha})\right]. \tag{24}$$

Krstić *et al.* [17] calculated numerically the energy poles from Eq. (24) in the case of elastic collisions ($\eta = 0$). However, such calculations cannot be performed without specifying the collision system. Instead of the energy pole, the θ pole is considered here, which is more appropriate for gaining general information on the resonance irrespective of the specific system. If Γ is very small, α may be assumed to be a real number in Eq. (24). Then, the θ pole can be given by

$$\theta_{\rm pol} = \theta_{\rm res} - i\,\Delta\theta, \tag{25}$$

where

$$\theta_{\rm res} = \theta(E_{\rm res}) = 2n\pi, \tag{26}$$

$$\Delta\theta = \frac{1}{2} \ln \frac{1 + e^{-2\pi\alpha}}{1 - P_0}. \tag{27}$$

Equation (26) is identical to Eq. (16), and gives the ridge position. In regard to Eq. (27), $2\Delta\theta$ may be interpreted as the width of the ridge peak along the θ direction on the topographical map $F(\alpha,\theta)$. One should define the actual ridge width $2\Delta\theta$ by equating $F(\alpha,\Delta\theta) = f(\alpha)/2$. Then, under the assumption of $\cos(\Delta\theta) = 1 - (\Delta\theta)^2/2$, one has

$$\Delta\theta = \frac{\sqrt{1 + e^{-2\pi\alpha}} - \sqrt{1 - P_0}}{[(1 + e^{-2\pi\alpha})(1 - P_0)]^{1/4}}, \tag{28}$$

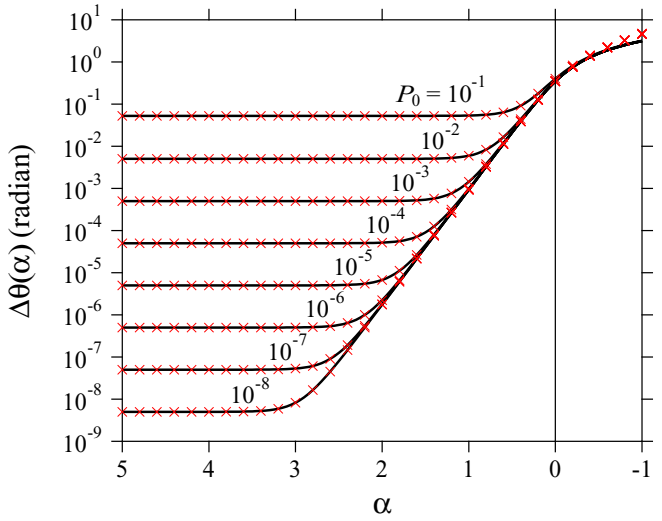

FIG. 6. Width functions $\Delta\theta(\alpha)$ in the range of $5 \geqslant \alpha \geqslant -1$ for the reactivities $P_0 = 10^{-8} - 10^{-1}$. Solid lines are Eq. (27), and crosses are Eq. (28).

which seems to be quite different from Eq. (27). However, from the numerical comparison between Eqs. (27) and (28) shown in Fig. 6, they turn out to be practically identical at least for $\alpha > 0$.

For a real collision problem, the resonance width must be measured along the energy-variation route $[\alpha(E),\theta(E)]$, which is not necessarily perpendicular to the ridge line. However, if $P_0 \ll 1$ and $\alpha > (2\pi)^{-1}$, the ridge width $2\Delta\theta$ is very narrow, as seen from Eq. (27) or (28), and then the peak width along the route is almost identical to $2\Delta\theta$ unless the route is nearly parallel to the ridge line [see Fig. 4(a)]. Hence, for very sharp resonances, it is expected that the energy width Γ is simply given by

$$\Gamma = 2\frac{dE}{d\theta}\Delta\theta. \tag{29}$$

If $|U| \ll |V|$, using Eq. (8) and neglecting ϕ yield

$$\hbar\frac{d\theta}{dE} = \frac{2m}{\hbar}\int_{R_0}^{R_1}\frac{dR}{k(R)}, \tag{30}$$

which is the classical period τ of the vibrational motion. Finally, the energy width is expressed as

$$\Gamma = \frac{2\hbar\Delta\theta}{\tau}. \tag{31}$$

The appearance of the vibrational period τ is reasonable. As τ becomes shorter, more frequently, the particle in the quasibound state hits the centrifugal barrier at $R = R_1$, or it stays longer in the reactive interaction zone $R < A$. This results in an increased incidence of barrier penetration or reaction. Since Eq. (27) can be written as

$$\Delta\theta = \Delta\theta_{\rm bar} + \Delta\theta_{\rm rea}, \tag{32}$$

where

$$\begin{aligned}\Delta\theta_{\rm bar} &= \tfrac{1}{2}\ln(1+e^{-2\pi\alpha}),\\ \Delta\theta_{\rm rea} &= \tfrac{1}{2}\left|\ln(1-P_0)\right|,\end{aligned} \tag{33}$$

one can partition the resonance width Γ into two physically important terms, i.e.,

$$\Gamma = \Gamma_{\rm bar} + \Gamma_{\rm rea}, \tag{34}$$

where $\Gamma_{\rm bar} = 2\hbar\Delta\theta_{\rm bar}/\tau$ is the width due to only the fragmentation through the (long-range) centrifugal potential and $\Gamma_{\rm rea} = 2\hbar\Delta\theta_{\rm rea}/\tau$ is due to only the reactive decay caused by the (short-range) interaction. The resonance width can be given analytically in terms of the QDT parameters for elastic collisions [18]. Compared to the QDT treatment, the present expression for the resonance width properly includes the effect of reactive channels and has a clear physical meaning also in appearance.

Figure 6 shows the width function $\Delta\theta(\alpha)$ for various reactivities P_0. In the limit $\alpha \to \infty$, the function $\Delta\theta(\alpha)$ becomes $\Delta\theta_{\rm rea}$ (or $P_0/2$ for $P_0 \ll 1$), which is independent of α. In other words, when the resonance energy is far below $E_{\rm BT}$, the resonance energy width in collisions is determined by only the reactive decay (i.e., $\Gamma = \Gamma_{\rm rea}$). With decreasing α, the width function $\Delta\theta$ is monotonically increasing from $\Delta\theta_{\rm rea}$, in accordance with the fact that the barrier penetration occurs more frequently. When $\alpha = \alpha_0$ (i.e., $P_{\rm res} = 1$), one has $\Delta\theta_{\rm bar} = \Delta\theta_{\rm rea}$ and hence $\Delta\theta = |\ln(1-P_0)|$ (or $\Delta\theta = P_0$ for $P_0 \ll 1$): the two energy widths due to the barrier penetration and due to the reactive decay just coincide ($\Gamma_{\rm bar} = \Gamma_{\rm rea}$). In the limit $\alpha \to -\infty$, the function $\Delta\theta(\alpha)$ becomes $\pi|\alpha|$, which is independent of P_0, although Eq. (29) may not be valid for $\alpha < 0$. In actual cases, the over-barrier resonances are usually very broad, and their widths are ill defined [see Fig. 4(d)].

D. Reaction rate constant

The reaction rate constant γ is given by

$$\gamma(T) = \langle v\sigma\rangle, \tag{35}$$

where T is the temperature, v is the initial velocity of the relative motion, and $\langle\cdot\rangle$ represents thermal averaging. In calculating the rate constant theoretically, one must take into account the resonance contribution, which sometimes makes a significant increment. However, when the resonance width is very narrow as in the case of the tunneling resonances, a search for such resonances becomes laborious in collision calculations. Therefore, it would be very useful if one could measure the importance of each resonance in the rate constant before carrying out collision calculations.

For the tunneling resonance occurring at $E = E_{\rm res} \ll E_{\rm BT}$, the contribution of the resonance to the cross section can be estimated in the form

$$\sigma_{\rm res}^{(i)}(E) = \left(\frac{\pi\hbar^2}{2mE}\right)\frac{(2L+1)P_{\rm res}^{(i)}[\Gamma^{(i)}/2]^2}{\left[E - E_{\rm res}^{(i)}\right]^2 + [\Gamma^{(i)}/2]^2}, \tag{36}$$

where i denotes each resonance. If the resonance is sufficiently sharp (i.e., $\Gamma \ll E_{\rm res}$), the resonance part of the rate constant becomes

$$\gamma_{\rm res}(T) = \frac{\hbar^2}{\sqrt{2}}\left(\frac{\pi}{mk_{\rm B}T}\right)^{3/2} \times \sum_i (2L+1)P_{\rm res}^{(i)}\Gamma^{(i)}\exp\left[-\frac{E_{\rm res}^{(i)}}{k_{\rm B}T}\right], \tag{37}$$

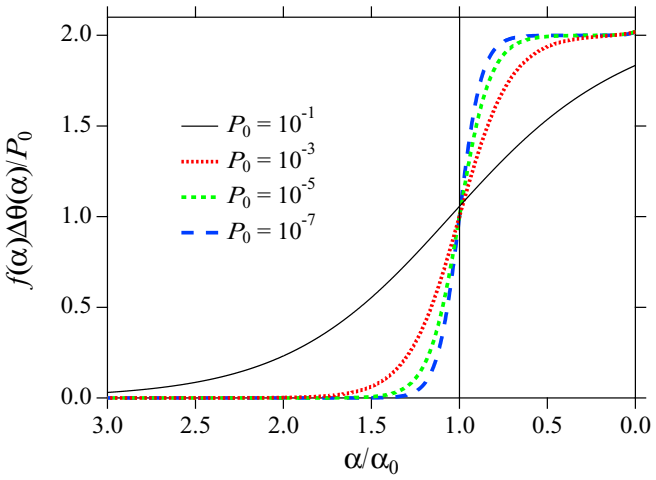

FIG. 7. Products $f(\alpha)\Delta\theta(\alpha)/P_0$ in the range of $3 \geqslant \alpha/\alpha_0 \geqslant 0$ for the reactivities $P_0 = 10^{-7}$–10^{-1}.

where k_B is the Boltzmann constant. Equation (37) suggests that the resonance contribution appears to be the product $P_{res}\Gamma$, namely, $f(\alpha_{res})\Delta\theta(\alpha_{res})/\tau$. Therefore, the importance of each resonance in the rate constant may be quickly measured by the magnitude of the universal quantity $f(\alpha_{res})\Delta\theta(\alpha_{res})$ without performing detailed QM collision calculations. Figure 7 shows $Q(\alpha) = f(\alpha)\Delta\theta(\alpha)/P_0$ as a function of α/α_0 for several reactivities P_0. Especially in the system with low reactivity, since the function $Q(\alpha)$ drops rapidly at $\alpha/\alpha_0 > 1$, it turns out that the resonances located at $\alpha \gg \alpha_0$ cannot contribute to a notable increment in the reaction rate constant.

Jachymski *et al.* [19] derived the effective reaction probability in which the increment due to the shape resonances is taken into account in an average sense. Following Jachymski *et al.* [19], the effective probability $\bar{P}(E,L)$ is given by averaging the probability function $F(\alpha,\theta,P_0)$ over θ:

$$\bar{P}(E,L) = \frac{1}{2\pi}\int_{-\pi}^{\pi} F(\alpha,\theta,P_0)d\theta = \frac{P_0}{1+e^{2\pi\alpha}P_0}. \quad (38)$$

The nonresonance part of the reaction probability may be given by [19,23,27]

$$P_{non}(E,L) = \frac{P_0}{1+e^{2\pi\alpha}}. \quad (39)$$

Then, the resonance contribution to the rate constant can be estimated by

$$\bar{\gamma}_{res}(T) = \langle v\bar{\sigma}_{res}\rangle, \quad (40)$$

where

$$\bar{\sigma}_{res}(E) = \frac{\pi\hbar^2}{2mE}\sum_L (2L+1)[\bar{P}(E,L) - P_{non}(E,L)]. \quad (41)$$

This expression is convenient because there is no need to identify each resonance.

III. SHAPE RESONANCES

A. $Li + H^+$ collisions

As a first example, the reaction processes in the $Li + H^+$ system are considered. In low-energy collisions of $Li + H^+$, nonradiative charge transfer becomes negligible, and notable reactive channels are radiative charge transfer and radiative association [28–30]:

$$Li + H^+ \rightarrow Li^+ + H + h\nu$$
$$\rightarrow LiH^+ + h\nu. \quad (42)$$

The chemistry of lithium is very important in the early universe [31–33], and the $Li + H^+$ collisions were investigated theoretically by several groups [28–30,34,35]. For this system, the potential curves of the relevant electronic states and the dipole moments are given in [29,36]. In the present study, the QM collision calculation has been carried out for energies $E = 0.001$–0.1 eV. The aim of the present paper is to perform a comprehensive analysis of shape resonances and to promote a better understanding of their systematics. Therefore, all the resonances over the reported energy range are, as a group, a matter of interest, and the results are offered only for the total radiative reaction (the branching ratio between the two radiative channels is not taken into account).

When the resonance occurs at an energy far below the barrier top E_{BT}, its peak width becomes very narrow, so that the resonance search cannot be made easily in the collision calculation. In the $Li + H^+$ system, the relative motion can be assumed to be substantially governed by only the local potential $V(R)$ because of $|U| \ll |V|$ [29,36]. In the present study, accordingly, a bound state, which is supported by the potential $V(R)$ plus an infinite wall artificially set at $R = R_{BT}$, was calculated quantum mechanically (referred to as the BS calculation), and its energy level ($E > 0$) was used as a guess at the peak position of the tunneling resonance. When $E \sim E_{BT}$ or $E > E_{BT}$, the resonance becomes broad, and its search can be made without any difficulty. The reaction probabilities $P(E,L)$ for each partial wave L and the reaction cross sections $\sigma(E)$ are presented in Fig. 1. About 120 resonances are associated with the related energy range. As mentioned previously, the QM calculation shows that the $Li + H^+$ system has very low reactivity, which is set to be $P_0 = \kappa = 10^{-5}$. The topographical map of $F(\alpha,\theta)$ for $P_0 = 10^{-5}$ is drawn in Fig. 4(a).

In Fig. 8(a), the heights P_{res} of the resonance peaks in $P(E,L)$ obtained by the QM calculation are plotted against the peak energy position E_{res}. The peak height undergoes very extensive changes from $<10^{-9}$ to ~ 1. It seems that regularity can hardly be found in this diagram. In Fig. 8(b), the peak heights are plotted against the tunneling parameter $\alpha_{res} = \alpha(E_{res})$ of the peak position. In this plot, all the peaks with heights with extremely different orders of magnitudes are beautifully arranged, and their heights lie nicely on a simple smooth curve, which is just the height function $f(\alpha)$ with $P_0 = 10^{-5}$. Thus, it has been demonstrated that the peak heights of the resonance probabilities in the QM calculation can be predicted by the simple closed-form expression derived from the WKB approximation. As seen in Fig. 8(b), several resonances occur at $\alpha_{res} \sim \alpha_0 = 1.832$, and accordingly, they have peak heights $P_{res} \sim 1$. When $\alpha_{res} < 6$, one can always find a clear peak structure in $P(E,L)$ corresponding to the level obtained by the BS calculation. This is probably true even for much larger α_{res} because the ridge in the topographical map remains prominent [i.e., $D(\alpha) \sim 16(P_0)^{-2}$] in the limit $\alpha \rightarrow \infty$.

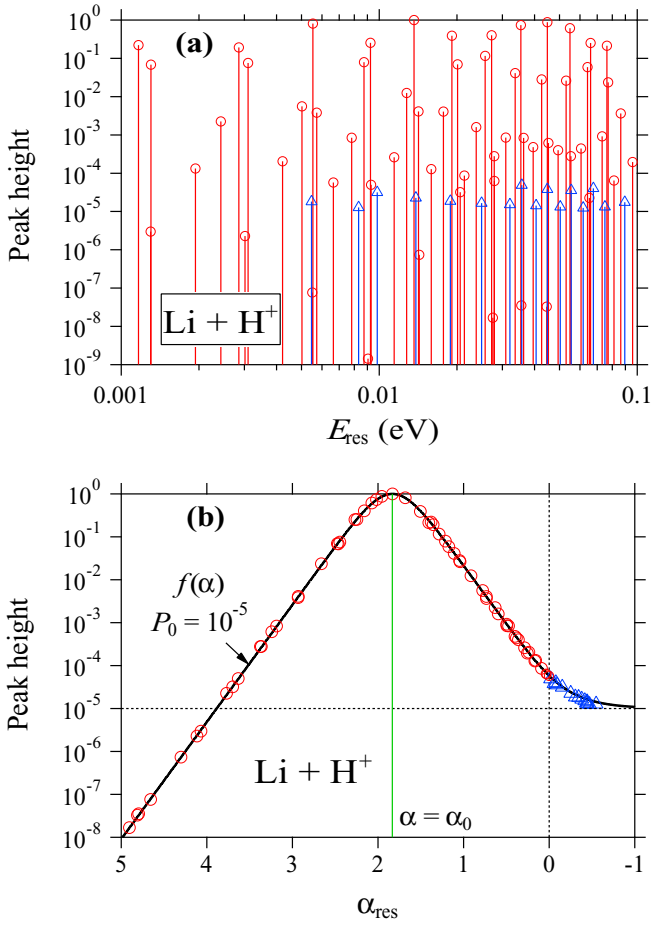

FIG. 8. Peak heights $P_{\rm res}$ of the resonances in the $\mathrm{Li}+\mathrm{H}^+$ reaction, obtained with the QM calculation, plotted (a) against the collision energy $E_{\rm res}$ of the resonance peak position and (b) against the tunneling parameter $\alpha_{\rm res}$ of the resonance peak position. Circles indicate the tunneling resonances ($\alpha_{\rm res} > 0$). Triangles indicate the over-barrier resonances ($\alpha_{\rm res} < 0$). The height function $f(\alpha)$, i.e., Eq. (18), for the reactivity $P_0 = 10^{-5}$ is shown by the solid line in (b).

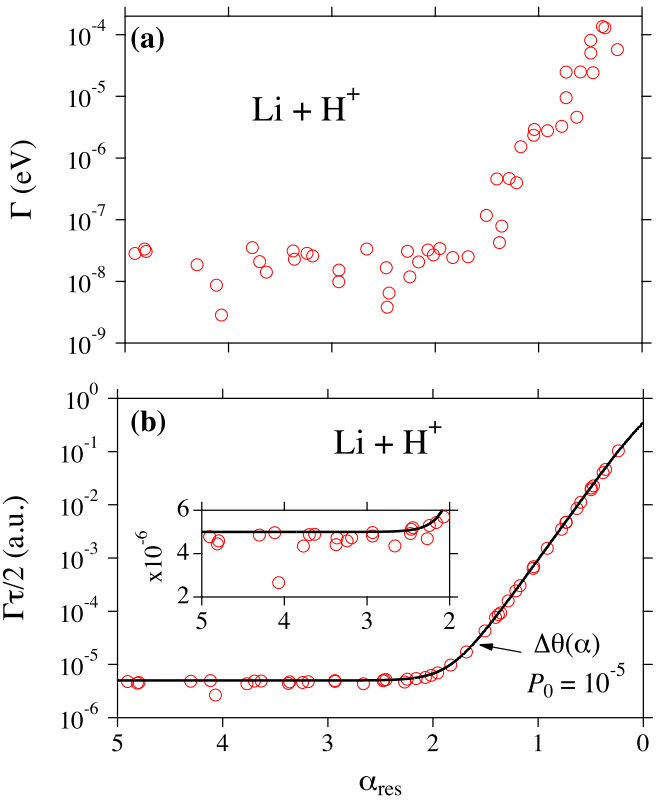

FIG. 9. (a) Energy widths Γ and (b) Γ times $\tau/2$ (τ is the vibrational period) of the resonances in the $\mathrm{Li}+\mathrm{H}^+$ reaction, obtained with the QM calculation (circles), plotted against the tunneling parameter $\alpha_{\rm res}$ of the resonance peak position. The width function $\Delta\theta(\alpha)$, i.e., Eq. (27), for the reactivity $P_0 = 10^{-5}$ is shown by the solid line in the (b). The insert in (b) is the linear-scale plot for $\alpha_{\rm res} \geqslant 2$.

However, the resonances located at $\alpha_{\rm res} > 6$ (compare with $\alpha_1 = 3.885$) have too low peak heights $P_{\rm res} < 10^{-9} \ll P_0$ and are discarded here. For over-barrier resonances located at $\alpha_{\rm res} < -0.5$, the peak height becomes only slightly larger than the background probability $P \simeq P_0 = 10^{-5}$. The peak structure of such resonances would be obscure. Therefore, the over-barrier resonances would be prominent only for $\alpha_{\rm res} \sim 0$, and the resonance search was not made for $\alpha_{\rm res} < -0.5$ in this study.

By assuming that the resonance profile has a Lorentz shape, one can derive the resonance energy width Γ from the reaction probabilities $P(E,L)$ in the QM calculation. When $\alpha_{\rm res} \sim 0$, however, it is not easy to obtain the resonance width unambiguously because the nonresonance part of $P(E,L)$ exhibits an abrupt change versus energy variation. In this study, the widths of the resonances located at $\alpha_{\rm res} < 0.1$ were not calculated. Figure 9(a) shows the QM results of the resonance widths Γ in the $\mathrm{Li}+\mathrm{H}^+$ reaction plotted against $\alpha_{\rm res}$. The widths shown in Fig. 9(a) undergo changes from $\sim 10^{-9}$ eV to $\sim 10^{-4}$ eV. It can be seen that Γ and $\alpha_{\rm res}$ have a high correlation, and hence, the plot of Γ versus $\alpha_{\rm res}$ is again right on target. Equation (31) further suggests that Γ times $\tau/(2\hbar)$ yields a universal quantity (i.e., $\Delta\theta$) which is a function of only α for a given P_0. In Fig. 9(b), the products $\Gamma\tau/2$ obtained in the QM calculation are plotted, and it is seen that the width function $\Delta\theta(\alpha)$ can mostly reproduce them. (The notable exception is the resonance at $\alpha_{\rm res} = 4.068$, and the reason is unknown.) When $\alpha_{\rm res} > 2$, as mentioned previously, the resonance width is determined by only the reactive (radiative) decay, and it seems that $\Gamma\tau/2$ in the QM calculation becomes independent of $\alpha_{\rm res}$.

Figure 7 suggests that the resonances located at $\alpha_{\rm res} \gg \alpha_0 = 1.832$ would be negligible in calculating the rate constant $\gamma(T)$ of the $\mathrm{Li}+\mathrm{H}^+$ reaction. Figure 10 shows the resonance part of the reaction rate constant calculated using Eq. (37) where the summation is taken over the resonances with $0.1 < \alpha_{\rm res}^{(i)} < \alpha_{\rm c}$: The convergence of the rate constant with respect to the cutoff parameter $\alpha_{\rm c}$ is investigated. The fact that the choice of $\alpha_{\rm c} = 2.5 = 1.36\alpha_0$ is sufficient for evaluating the resonance contribution is in accordance with the findings in Fig. 7. The nonresonance part of the reaction rate constant for $\mathrm{Li}+\mathrm{H}^+$ is roughly given by $\kappa\gamma_{\rm L} = 1.22 \times 10^{-13}$ cm^3/s, with $\gamma_{\rm L}$ being the Langevin rate constant. Therefore, owing

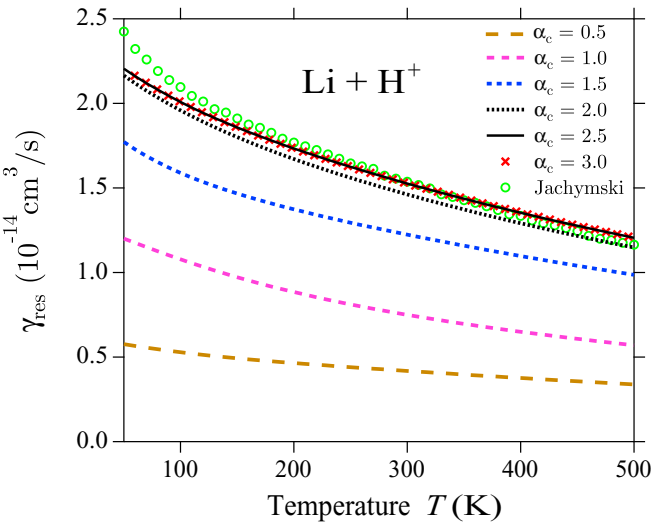

FIG. 10. Increments in the reaction rate constant $\gamma_{\rm res}(T)$, i.e., Eq. (37), attributed to all the tunneling resonances with $\alpha_{\rm res} \in (0.1,\alpha_{\rm c})$ in $\mathrm{Li} + \mathrm{H}^+$ as a function of the temperature T. The cutoff parameter $\alpha_{\rm c}$ is varied between 0.5 and 3.0. Resonance contributions $\bar{\gamma}_{\rm res}(T)$ obtained using Eq. (38) of Jachymski *et al.* [19] are also shown.

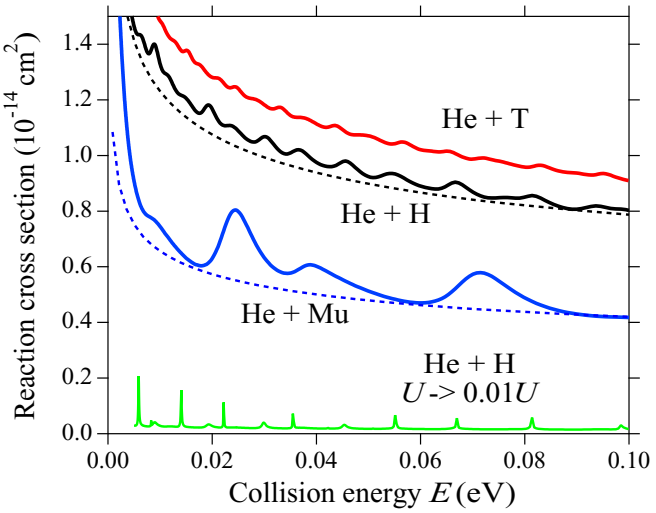

FIG. 11. Reaction cross sections $\sigma(E)$ in collisions of $\mathrm{He}(2\,^3S)$ with Mu, H, and T, obtained with the QM calculation. Also shown is the result for the hypothetical $\mathrm{He}(2\,^3S) + \mathrm{H}$ system, in which the reactive interaction U is replaced with $0.01U$. Dashed lines indicate the classical reaction cross sections $\kappa\sigma_0$, with $\kappa = 0.75$ for $\mathrm{He} + \mathrm{H}$ and with $\kappa = 0.40$ for $\mathrm{He} + \mathrm{Mu}$.

to the effect of the tunneling resonances, the rate constant increases by 10%–20% at the temperatures shown in Fig. 10. About half of the resonances treated in the present calculation have $\alpha_{\rm res} < 1.36\alpha_0$ and contribute to such increments. The resonance contribution $\bar{\gamma}_{\rm res}(T)$ obtained using Eq. (41) with $\alpha > 0$ is also plotted in Fig. 10, and good agreement is obtained with the present directly calculated result except at very low temperatures. Since the number of resonances contributing to the rate constant is smaller at lower temperatures, the averaging over θ in Eq. (38) is not appropriate for a reliable estimate at very low temperatures.

B. $\mathrm{He}(2\,^3S) + \mathrm{H}$ collisions

A second example is the $\mathrm{He}(2\,^3S) + \mathrm{H}$ system, which has two autoionization channels of Penning ionization and associative ionization:

$$\begin{aligned} \mathrm{He}(2\,^3S) + \mathrm{H} &\to \mathrm{He} + \mathrm{H}^+ + e \\ &\to \mathrm{HeH}^+ + e. \end{aligned} \tag{43}$$

This is the simplest and most fundamental among the various systems bringing about Penning ionization and was hence intensively investigated both theoretically and experimentally [25,37–42]. In the present study, by using the latest version of the complex potential energy curve of $\mathrm{He}(2\,^3S) + \mathrm{H}$ [42], the QM collision calculation was carried out for energies $E = 0.005$–0.1 eV. As in Sec. III A, the results are presented only for the total autoionization reaction.

Figure 11 shows the reaction cross sections $\sigma(E)$ in $\mathrm{He}(2\,^3S) + \mathrm{H}$ and also in its isotope systems $\mathrm{He}(2\,^3S) + \mathrm{Mu}$ and $\mathrm{He}(2\,^3S) + \mathrm{T}$. It is seen that the reaction cross section becomes larger for heavier reduced mass m. This fact is clearly reflected in the classical reaction cross section $\kappa\sigma_0$: The reaction efficiency is $\kappa = 0.40, 0.75$ and 0.88 for Mu, H, and T, respectively, whereas σ_0 is independent of m. The mass dependence may be explained by a semiclassical method [37]; namely, $\kappa \simeq P_0 \sim 1 - \exp(-c\sqrt{m})$, where c is a constant independent of m. The $\mathrm{He}(2\,^3S) + \mathrm{H}$ system is an example with high reaction efficiency, and the isotope $\mathrm{He}(2\,^3S) + \mathrm{Mu}$ system can offer lower reaction efficiency. Compared to those of the $\mathrm{Li} + \mathrm{H}^+$ system, the cross sections have a much less complicated energy dependence and show a structure like undulation (rather than peaks) due to resonances. It is expected that no notable tunneling resonances occur for $P_0 > 2(\sqrt{2} - 1) = 0.8284$ [23]. The $\mathrm{He}(2\,^3S) + \mathrm{T}$ system is such a case. Another similar example is the exotic reaction $\bar{p} + \mathrm{H} \to \bar{p}p + e$ ($P_0 \simeq 0.9$), with $\bar{p}$ being an antiproton, which was studied in [43]. For both $\bar{p} + \mathrm{H}$ [43] and $\mathrm{He}(2\,^3S) + \mathrm{T}$, the QM calculations show indeed that no clear peak structure to be attributed to the tunneling resonance is found. In the $\mathrm{He}(2\,^3S) + \mathrm{H}$ and $\mathrm{He}(2\,^3S) + \mathrm{Mu}$ systems, since $\kappa < 2(\sqrt{2} - 1)$, a certain number of tunneling resonances are expected to be observable. The present study considers these two systems and additionally the hypothetical $\mathrm{He}(2\,^3S) + \mathrm{H}$ system which has $\kappa = 0.012$ by replacing the reactive interaction U with $0.01U$. The reactivity is set to be $P_0 = \kappa$ also in these systems. (See Fig. 3 for the L dependence.) Topographical maps of $F(\alpha,\theta)$ similar to the present cases of not too low reactivities are drawn in paper I and would be of some help.

Figure 12 shows the reaction probabilities $P(E,L)$ in $\mathrm{He}(2\,^3S) + \mathrm{H}$ for all the partial waves L associated with the collision energies $0.005 \leqslant E \leqslant 0.1$ eV. Although the reduced masses of $\mathrm{He}(2\,^3S) + \mathrm{H}$ and $\mathrm{Li} + \mathrm{H}^+$ are mostly the same, fewer partial waves contribute to the $\mathrm{He}(2\,^3S) + \mathrm{H}$ reaction because the long-range attractive force is much weaker in $\mathrm{He}(2\,^3S) + \mathrm{H}$. In Fig. 13, the heights of the resonance peaks observed in Fig. 12 are plotted against the tunneling parameter $\alpha_{\rm res}$ of the peak position. The data are, overall, reproduced by the height function $f(\alpha)$ with $P_0 = 0.75$, which has a maximum ($f = 1$) at $\alpha = \alpha_0 = -0.1749 < 0$. (The peak

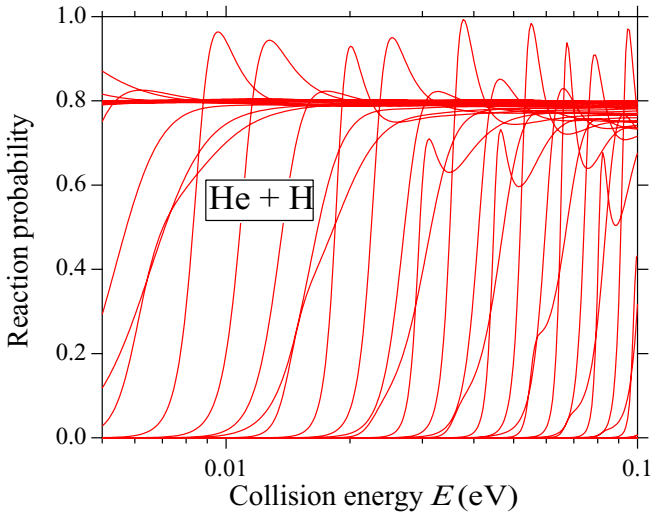

FIG. 12. Reaction probabilities $P(E,L)$ in He($2\,^3S$) + H collisions for $L = 0$–38, obtained with the present QM calculation, are shown at collision energies $E = 0.005$–0.1 eV.

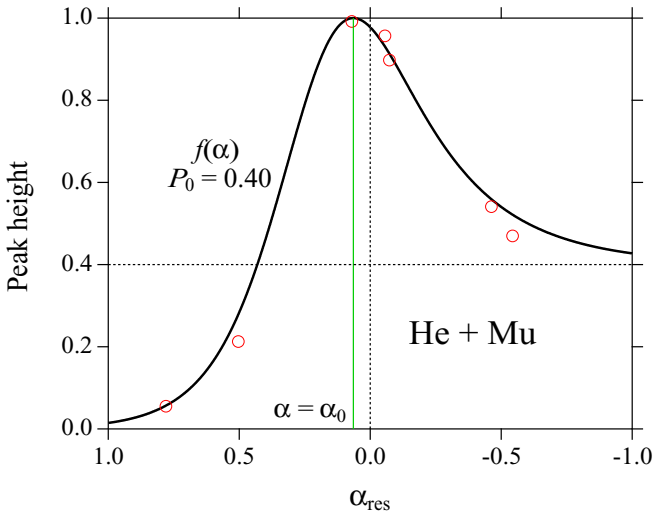

FIG. 14. Peak heights P_{res} of the resonances in the reaction obtained with the QM calculation (circles) for the He($2\,^3S$) + Mu system. The height function $f(\alpha)$, i.e., Eq. (18), for the reactivity $P_0 = 0.40$ is shown by the solid line.

heights in Fig. 13 are plotted in a linear scale, whereas those in Fig. 8 are in a log scale.) In contrast to the Li + H^+ case ($P_0 \ll 1$), the QM calculation shows that only a few resonance peaks can be observed for $\alpha_{res} > 0$. This can be directly attributed to negative α_0: the peak height becomes extremely small ($P_{res} \ll P_0$) for the resonances occurring at $\alpha_{res} \gg \alpha_0$ (compare with $\alpha_1 = 0.09157$). Of course, the most prominent resonances that have peak heights $P_{res} \sim 1$ are the over-barrier type in He($2\,^3S$) + H. Thus, it can be concluded that the over-barrier type is a dominant resonance process if the reaction system has $\alpha_0 < 0$. Incidentally, the He($2\,^3S$) + T system has $\alpha_0 = -0.3171$ and $\alpha_1 = -0.07612$.

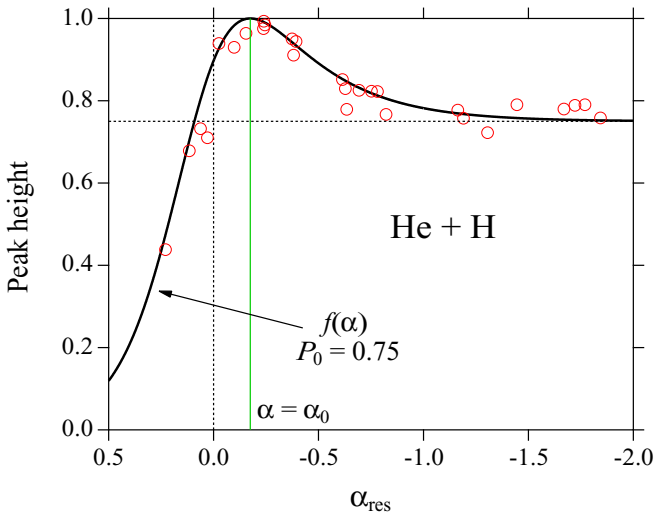

FIG. 13. Peak heights P_{res} of the resonances in the reaction obtained with the QM calculation (circles) for the He($2\,^3S$) + H system. The resonances appearing as a shoulder structure are not shown. The height function $f(\alpha)$, i.e., Eq. (18), for the reactivity $P_0 = 0.75$ is shown by the solid line.

As a trial, the BS calculation was carried out for the investigation of the tunneling resonances ($\alpha_{res} > 0$) also in the He($2\,^3S$) + H collisions. It should be remembered, however, that the local potential $V(R)$ might not be valid for the relative motion at $R < A$ unless $P_0 \ll 1$. The BS calculation offers in total 31 quasibound levels at energies $0.005 \leqslant E \leqslant 0.1$ eV. Of these, two levels located at $\alpha < 0.5$ are found to correspond to peaks ($\alpha_{res} = 0.1158$ and 0.2294) in $P(E,L)$, and ten levels at $\alpha \lesssim 1.5$ are found to be associated with shoulders in $P(E,L)$ (see Fig. 12). Unfortunately, the shoulder structure is less remarkable for resonance effects, and the heights of shoulders are ill defined. Accordingly, the shoulder data are not added in Fig. 13. All the other levels in the BS calculation have $\alpha \gtrsim 1.5$, and no signs of being resonances can be practically discovered in $P(E,L)$ corresponding to these BS levels. It is expected that any distinctive appearance of the resonance effect will be missing for large α if P_0 is smaller than but comparable to $2(\sqrt{2}-1)$.

Figure 13 shows that two peaks are located at $\alpha_{res} = 0.02930$ and 0.06201, which cannot be predicted by the BS calculation. They might be considered to be due to orbiting resonances because $\alpha_{res} \sim 0$ [17]. (The same situation arises also in the Li + H^+ reaction; three peaks at $\alpha_{res} = 0.002224, 0.02990$, and 0.03883 should be identified as orbiting resonances.) It is a delicate point whether the BS calculation is functional for the prediction of orbiting resonances. However, the orbiting resonance is usually broad, and its search is not very difficult in the collision calculation.

The He($2\,^3S$) + Mu system ($P_0 = 0.40$) has $\alpha_0 = 0.06453$. Figure 14 shows the peak heights of the resonance probabilities in this isotope system. Because of light reduced mass, only a small number of resonances can be observed in total. The peak heights of these resonances can be reproduced by $f(\alpha)$ with $P_0 = 0.40$. The BS calculation predicts nine tunneling resonances at energies $0.005 \leqslant E \leqslant 0.1$ eV. Actually, three levels in the BS calculation are associated with one shoulder

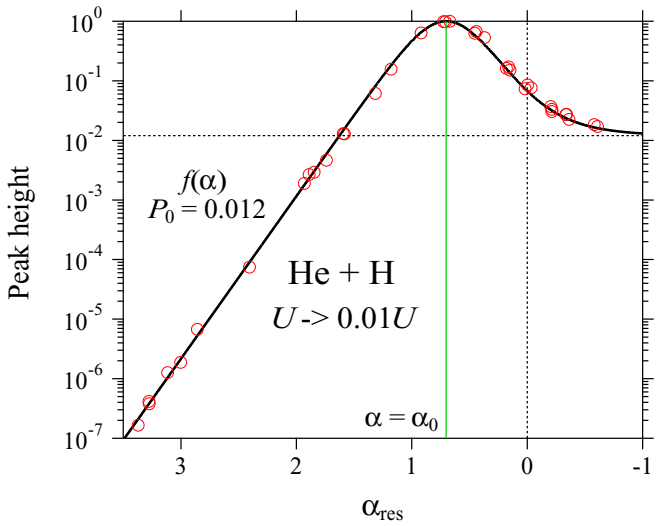

FIG. 15. Peak heights P_{res} of the resonances in the reaction obtained with the QM calculation (circles) for the hypothetical He($2\,^3S$) + H system, in which the reactive interaction U is replaced with $0.01U$. The height function $f(\alpha)$, i.e., Eq. (18), for the reactivity $P_0 = 0.012$ is shown by the solid line.

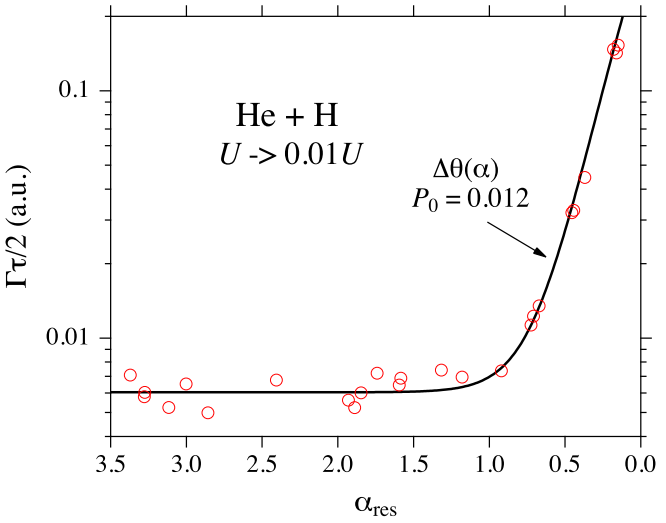

FIG. 16. Energy widths Γ times $\tau/2$ of the resonances in the reaction obtained with the QM calculation (circles) for the hypothetical He($2\,^3S$) + H system, in which the reactive interaction U is replaced with $0.01U$. The width function $\Delta\theta(\alpha)$, i.e., Eq. (27), for the reactivity $P_0 = 0.012$ is shown by the solid line.

and two peaks ($\alpha_{res} = 0.5034$ and 0.7801) in $P(E,L)$. For the other BS levels, which are located at $\alpha > 2$ (i.e., $\alpha \gg \alpha_1 = 0.4310$), the resonances are practically negligible (although shoulder structures with $P \lesssim 10^{-5}$ can be found). The peak at $\alpha_{res} = 0.07019$ is not predicted by the BS calculation and should be regarded as the orbiting resonance. Since $\alpha_0 > 0$ in the He($2\,^3S$) + Mu system, the relative ratio of the identified tunneling resonances is larger than that in He($2\,^3S$) + H. Furthermore, since $\alpha_0 \sim 0$, only the orbiting resonance can satisfy $\alpha_{res} \simeq \alpha_0$, and hence, $P_{res} \simeq 1$.

The hypothetical He($2\,^3S$) + H system ($P_0 = 0.012$) has $\alpha_0 = 0.7020$. Figure 15 shows the peak heights of the resonance probabilities, which can be reproduced by $f(\alpha)$ with $P_0 = 0.012$. Since $P_0 \ll 1$ and $\alpha_0 \simeq 1$, a lot more tunneling resonances appear to be prominent than in the original He($2\,^3S$) + H system. As in the case of Li + H^+, all the resonances with $P_{res} \sim 1$ are the tunneling type, and the peak structure is clearly observed even when P_{res} becomes very small. Probably, all the BS levels could be associated with peaks in $P(E,L)$: The ridge in the topographical map is sufficiently steep even for large α. When $\alpha > 3.5$ (compare with $\alpha_1 = 1.627$), however, the corresponding peaks have $P_{res} < 10^{-7} \ll P_0$, and such resonances are practically negligible in the reaction process. For the resonances with $\alpha_{res} > 0$, only the peak at $\alpha_{res} = 0.01852$ cannot be predicted by the BS calculation. In Fig. 15, there are two peaks located at negative values of $\alpha_{res} \sim 0$ (i.e., $\alpha_{res} = -0.002578$ and -0.03413); it may be allowable to identify these resonances as the orbiting (rather than over-barrier) type. Considering the previous results reported in this paper, it seems feasible that the resonances located at $|\alpha_{res}| \lesssim 0.1$ are classified as the orbiting type.

In the case of $P_0 \ll 1$, the energy width of the tunneling resonance should be estimated by Eq. (31). Figure 16 shows $\Gamma\tau/2$ in the hypothetical He($2\,^3S$) + H system. The width function $\Delta\theta(\alpha)$ with $P_0 = 0.012$ is also plotted. The agreement between the QM results and $\Delta\theta(\alpha)$ seems to be not as good as for Li + H^+. This is probably because the variation rate of P_0 with L is more rapid for hypothetical He($2\,^3S$) + H than for Li + H^+ (see Fig. 3) or because the reactivity $P_0 = 0.012$ may not be sufficiently small to assume Eq. (29). Nevertheless, an overall picture of the α_{res} dependence can be explained by the width function $\Delta\theta(\alpha)$. For $\alpha_{res} > 1$, the product $\Gamma\tau/2$ becomes roughly independent of α_{res} in the hypothetical He($2\,^3S$) + H system.

IV. SUMMARY AND CONCLUSION

A comprehensive way of looking at the vast variety of shape resonances in low-energy exoergic reactive collisions and how to arrange them properly have been proposed. The reaction systems investigated as examples were He($2\,^3S$) + H, He($2\,^3S$) + Mu, hypothetical He($2\,^3S$) + H, and Li + H^+. The related processes are the autoionization reaction in the first three systems and the radiative reaction in the last system. The reaction processes are characterized by the reactivity P_0, which can be mostly set to be identical to the reaction efficiency κ. These systems have the reactivities $P_0 = 0.75$, 0.40, 0.012, and 10^{-5}, respectively.

The shape resonances should be arranged according to the magnitude of the tunneling parameter α. The resonances might be classified as a tunneling type if $\alpha \gtrsim 0.1$, an orbiting type if $|\alpha| \lesssim 0.1$, and an over-barrier type if $\alpha \lesssim -0.1$.

Simple universal formulas, which can be derived from the WKB approximation, are found to be beneficial to the systematical understanding of the shape resonances. The probability peak heights of the resonances and the energy widths of the tunneling resonances can be predicted by the height function $f(\alpha)$ and the width function $\Delta\theta(\alpha)$, which are dependent only on α for a given reactivity P_0. The resonance width can be expressed as the sum of the barrier penetration

and reactive decay widths, and this explains the α dependence of the width.

The reaction probability at a resonance energy always becomes $P \simeq 1$ when the tunneling parameter corresponding to this energy is $\alpha \simeq \alpha_0 = (2\pi)^{-1} \ln[(1 - P_0)/P_0]$. The physical meaning of this condition is that the transmission coefficient is nearly equal to the reactivity P_0 at this energy or, for the tunneling resonance, that the barrier penetration width is nearly the same as the reactive decay width. This conclusion is always true no matter how low the reactivity P_0 is. The resonance occurring at $\alpha \gg \alpha_0$ has a negligible profile or a very small peak height ($P_{\rm res} \ll P_0$) and actually plays no role in the reaction process. The over-barrier resonance becomes less important at $|\alpha| > 1$.

In the reaction system, the relative importance between the over-barrier and the tunneling resonances changes according to the reactivity P_0 (or α_0). In the system with $P_0 \gtrsim 0.5$ (i.e., $\alpha_0 \lesssim 0$), the over-barrier resonances play a major role. In the system with $P_0 \ll 1$ (or $\alpha_0 \gtrsim 1$), the tunneling resonances occur overwhelmingly.

For application, knowing to what extent the shape resonances should be taken into account in the calculation of the reaction rate constants is of great interest. The contribution of the resonance is proportional to the peak height times the peak width, which can be evaluated from the product $f(\alpha)\Delta\theta(\alpha)$ without carrying out detailed collision calculations. The present study indicates that only the resonances located at $\alpha \lesssim \alpha_0$ are important in the calculation of the rate constants if the system has $P_0 \ll 1$.

ACKNOWLEDGMENTS

This work was supported by JSPS KAKENHI Grant No. 15H03753.

[1] D. W. Chandler, J. Chem. Phys. **132**, 110901 (2010).
[2] M. Konrad and F. Linder, J. Phys. B **15**, L405 (1982).
[3] H. M. J. M. Boesten, C. C. Tsai, B. J. Verhaar, and D. J. Heinzen, Phys. Rev. Lett. **77**, 5194 (1996).
[4] H. M. J. M. Boesten, C. C. Tsai, J. R. Gardner, D. J. Heinzen, and B. J. Verhaar, Phys. Rev. A **55**, 636 (1997).
[5] R. Côté, A. Dalgarno, A. M. Lyyra, and Li Li, Phys. Rev. A **60**, 2063 (1999).
[6] T. Volz, S. Dürr, N. Syassen, G. Rempe, E. van Kempen, and S. Kokkelmans, Phys. Rev. A **72**, 010704(R) (2005).
[7] S. Chefdeville, T. Stoecklin, A. Bergeat, K. M. Hickson, C. Naulin, and M. Costes, Phys. Rev. Lett. **109**, 023201 (2012).
[8] A. B. Henson, S. Gersten, Y. Shagam, J. Narevicius, and E. Narevicius, Science **338**, 234 (2012).
[9] S. Chefdeville, Y. Kalugina, S. Y. T. van de Meerakker, C. Naulin, F. Lique, and M. Costes, Science **341**, 1094 (2013).
[10] S. N. Vogels, J. Onvlee, S. Chefdeville, A. van der Avoird, C. Groenenboom, and S. Y. T. van de Meerakker, Science **350**, 787 (2015).
[11] J. Jankunas, K. Jachymski, M. Hapka, and A. Osterwalder, J. Chem. Phys. **142**, 164305 (2015).
[12] M. Beyer and F. Merkt, Phys. Rev. Lett. **116**, 093001 (2016).
[13] R. D. Levine and R. B. Bernstein, in *Molecular Reaction Dynamics* (Clarendon, Oxford, 1974), Chap. 2.
[14] K. W. Ford, D. L. Hill, M. Wakano, and J. A. Wheeler, Ann. Phys. (NY) **7**, 239 (1959).
[15] J. N. L. Connor, Mol. Phys. **15**, 37 (1968).
[16] M. S. Child, in *Semiclassical Mechanics with Molecular Applications* (Clarendon, Oxford, 1991), Chap. 3.
[17] P. S. Krstić, J. H. Macek, S. Yu. Ovchinnikov, and D. R. Schultz, Phys. Rev. A **70**, 042711 (2004).
[18] B. Gao, Phys. Rev. Lett. **104**, 213201 (2010).
[19] K. Jachymski, M. Krych, P. S. Julienne, and Z. Idziaszek, Phys. Rev. A **90**, 042705 (2014).
[20] M. Li, L. You, and B. Gao, Phys. Rev. A **89**, 052704 (2014).
[21] B. E. Londoño, J. E. Mahecha, E. Luc-Koenig, and A. Crubellier, Phys. Rev. A **82**, 012510 (2010).
[22] H. da Silva, Jr., M. Raoult, M. Aymar, and O. Dulieu, New J. Phys. **17**, 045015 (2015).
[23] K. Sakimoto, J. Phys. B **47**, 025201 (2014).
[24] B. Zygelman and A. Dalgarno, Phys. Rev. A **38**, 1877 (1988).
[25] P. E. Siska, Rev. Mod. Phys. **65**, 337 (1993).
[26] J. C. Light and R. B. Walker, J. Chem. Phys. **65**, 4272 (1976).
[27] S. C. Miller, Jr., and R. H. Good, Jr., Phys. Rev. **91**, 174 (1953).
[28] M. Kimura, C. M. Dutta, and N. Shimakura, Astrophys. J. **430**, 435 (1994); **454**, 545 (1995).
[29] A. Dalgarno, K. Kirby, and P. C. Stancil, Astrophys. J. **458**, 397 (1996).
[30] P. C. Stancil and B. Zygelman, Astrophys. J. **472**, 102 (1996).
[31] S. Lepp, P. C. Stancil, and A. Dalgarno, J. Phys. B **35**, R57 (2002).
[32] E. Bodo, F. A. Gianturco, and R. Martinazzo, Phys. Rep. **384**, 85 (2003).
[33] D. Galli and F. Palla, Annu. Rev. Astron. Astrophys. **51**, 163 (2013).
[34] F. A. Gianturco and P. Gori Giorgi, Astrophys. J. **479**, 560 (1997).
[35] I. Baccarelli, L. Andtric, T. P. Grozdanov, and R. McCarroll, J. Chem. Phys. **117**, 3013 (2002).
[36] H. Berriche and F. X. Gadea, Chem. Phys. **191**, 119 (1995).
[37] W. H. Miller, C. A. Slocomb, and H. F. Schaefer, III, J. Chem. Phys. **56**, 1347 (1972).
[38] A. P. Hickman and H. Morgner, J. Chem. Phys. **67**, 5484 (1977).
[39] R. J. Bieniek, Phys. Rev. A **18**, 392 (1978).
[40] H. Waibel, M.-W. Ruf, and H. Hotop, Z. Phys. D **9**, 191 (1988).
[41] A. Merz, M.-W. Ruff, H. Hotop, M. Movre, and W. Meyer, J. Phys. B **27**, 4973 (1994).
[42] M. Movre and W. Meyer, J. Chem. Phys. **106**, 7139 (1997).
[43] K. Sakimoto, Phys. Rev. A **88**, 012507 (2013).